

Diversify, Don't Fine-Tune: Scaling Up Visual Recognition Training with Synthetic Images

Zhuoran Yu^{1*} Chenchen Zhu² Sean Culatana² Raghuraman Krishnamoorthi²
 Fanyi Xiao^{2†} Yong Jae Lee^{1†}
¹University of Wisconsin-Madison ²Meta

Abstract

Recent advances in generative deep learning have enabled the creation of high-quality synthetic images in text-to-image generation. Prior work shows that fine-tuning a pretrained diffusion model on ImageNet and generating synthetic training images from the finetuned model can enhance an ImageNet classifier's performance. However, performance degrades as synthetic images outnumber real ones. In this paper, we explore whether generative fine-tuning is essential for this improvement and whether it is possible to further scale up training using more synthetic data. We present a new framework leveraging off-the-shelf generative models to generate synthetic training images, addressing multiple challenges: class name ambiguity, lack of diversity in naive prompts, and domain shifts. Specifically, we leverage large language models (LLMs) and CLIP to resolve class name ambiguity. To diversify images, we propose contextualized diversification (CD) and stylized diversification (SD) methods, also prompted by LLMs. Finally, to mitigate domain shifts, we leverage domain adaptation techniques with auxiliary batch normalization for synthetic images. Our framework consistently enhances recognition model performance with more synthetic data, up to 6x of original ImageNet size showcasing the potential of synthetic data for improved recognition models and strong out-of-domain generalization.

1. Introduction

Recent advances in denoising probabilistic diffusion models [13, 23, 24, 36, 45] have excelled in generating photo-realistic synthetic images in open-vocabulary text-to-image generation [35, 42, 45, 46, 57]. These capabilities stem from large-scale image-text datasets like LAION [48, 49] and multimodal models like CLIP [41]. Ongoing research explores the potential of using synthetic images from such

*work partially done during internship at Meta.

†equal advising.

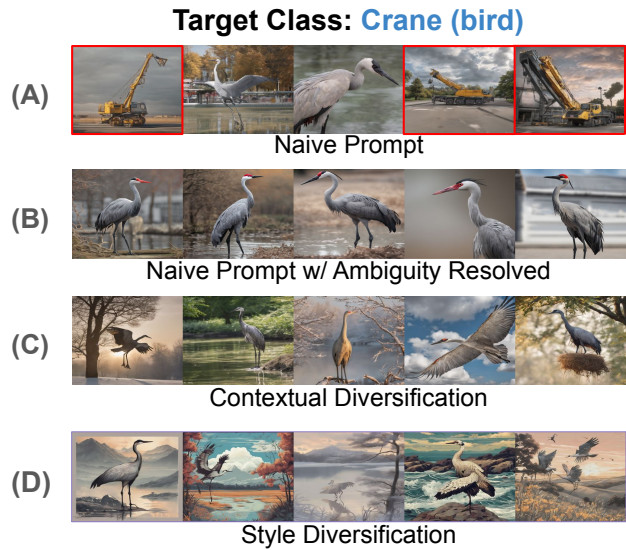


Figure 1. **Prompt augmentation for unambiguous and diversified synthetic data generation.** We improve synthetic data generation by augmenting prompts from two perspectives: 1) we resolve the ambiguity for class names to avoid generating images with incorrect semantics for the target class (e.g., row A vs. B), and 2) we diversify the prompts used to generate synthetic images both in terms of their contexts (row C) and styles (row D). We achieve both augmentations by leveraging the power of LLMs.

diffusion models to improve recognition models [2, 20, 47], mostly in scenarios with low-shot real training images. Critically, whether such synthetic images can improve a recognition model's performance when real images at the ImageNet-scale are already available remains an open research question.

Recent work [2] that tries to answer this question delved into the intricate process of fine-tuning the open-vocabulary Imagen [46] diffusion model on ImageNet [12] and using it to generate synthetic images conditioned on ImageNet class labels. However, fine-tuning adds an extra layer of complexity in designing the fine-tuning strategy while also requiring additional resources for training. Moreover, when

applying to diverse datasets, this practice requires repeating the fine-tuning process for each dataset, significantly increasing overall complexity and costs. These challenges prompt us to ask: *Is it necessary to finetune a diffusion model in order to generate useful synthetic training data to improve a recognition model’s performance on ImageNet-scale datasets?*

In this paper, we provide an initial attempt in answering this question. Instead of fine-tuning a pretrained open-vocabulary diffusion model, we leverage a frozen off-the-shelf one to generate additional training images when there is already a large-scale training set.

One typical approach to achieving this would be to employ the naive prompt format *a photo of a {class name}* and train the recognition model with a combination of real and synthetic images. However, several notable challenges arise from this simple approach from both the data generation and model training aspects, which lead to sub-optimal recognition performance.

Synthetic Data Generation. Datasets such as ImageNet often contain class names that have multiple meanings. For instance, *crane* can denote both a construction machine and a bird species. These divergent interpretations can lead to unintended semantic misalignment between synthetic images and class semantics such as generating machine images for a class of bird cranes. Furthermore, adhering to a fixed prompt format can lead to redundancy in the generated images, where most of them exhibit similar visual characteristics. The limited diversity in synthetic images exacerbates the risk of the recognition model overfitting to such images, thereby leading to challenges when scaling up training with synthetic data.

We address these challenges by redesigning the data generation pipeline to solve the label ambiguity and generate diversified images, with the assistance of large language models (LLMs). While existing approaches leverage dataset-specific hierarchical information [47] or manually process class names [41] to resolve the ambiguity in class names, we propose a general solution that requires minimal human effort. Specifically, we query LLMs to extract multiple meanings of each class name and select the meaning with the highest CLIP [41] image-text similarity associated with the actual real images of the class. The selected meaning is used as an additional explanation of the class name in the synthetic data generation process.

Next, we generate diversified synthetic images by formulating generation prompts using the knowledge from LLMs. We introduce two distinct methods for diversification: *contextualized diversification (CD)* and *stylized diversification (SD)*, each based on different principles. CD aims to generate photo-realistic synthetic images featuring class *c* with diversity introduced through contextual foreground and background objects. In contrast, SD emphasizes the

generation of images with varying styles. This whole process of obtaining generation prompts is realized by prompting LLMs, minimizing the need for human labor.

Domain Shifts in Recognition Model Training. Another inherent challenge arises from the domain shifts between real and synthetic images. Even though recent diffusion models produce synthetic images of higher quality, they still bear a different distribution as manifested by their separable features within the feature space [38]. When synthetic images start to dominate the real images in recognition model training, the domain shifts can lead to suboptimal performance if not properly handled.

We view real and synthetic images as being from two separate domains, and propose to mitigate the domain shifts between them by drawing inspiration from domain adaptation literature. First, we introduce auxiliary batch normalization layers (BN) [8, 32, 50] for recognition models that employ BN to process synthetic images. We further adjust domain-level sampling weights ensuring each batch contains a roughly equal number of real and synthetic images during training, avoiding overfitting to synthetic images.

Main Contributions. Through our refined design of the synthetic data generation pipeline and mitigation of domain gaps, our framework yields significant performance improvements over using fine-tuned generative models [2] on ImageNet classification. For example, with ResNet-50, our method achieves +2.53% accuracy improvement over the baseline that is trained with real images only, and +1.10% compared to the model trained with real and synthetic images from finetuned Imagen [2].

Interestingly, with our simpler framework (*i.e.*, no generative finetuning), our framework consistently enhances results, even when scaling up synthetic data to 6x the original training dataset size. This is in stark contrast to prior generative finetuning work [2], which observed that recognition performance degrades as the synthetic images outnumber real ones in training. This boldly underscores the untapped potential of synthetic data at a larger scale. Additionally, models trained with synthetic images from our framework also show more robust performance in out-of-domain generalization. Specifically, a ResNet-50 trained with ImageNet real images and synthetic images from our framework demonstrate +2.89%, +7.55%, and +5.77% absolute accuracy improvement on ImageNet-V2 [43], ImageNet-Sketch [54], and ImageNet-Rendition [21], respectively; with vision transformers, the improvements on ImageNet-Sketch and Rendition can even exceed +10%.

2. Related Work

Diffusion Models for Image Generation. Diffusion models [51] have been widely applied in image generation [13,

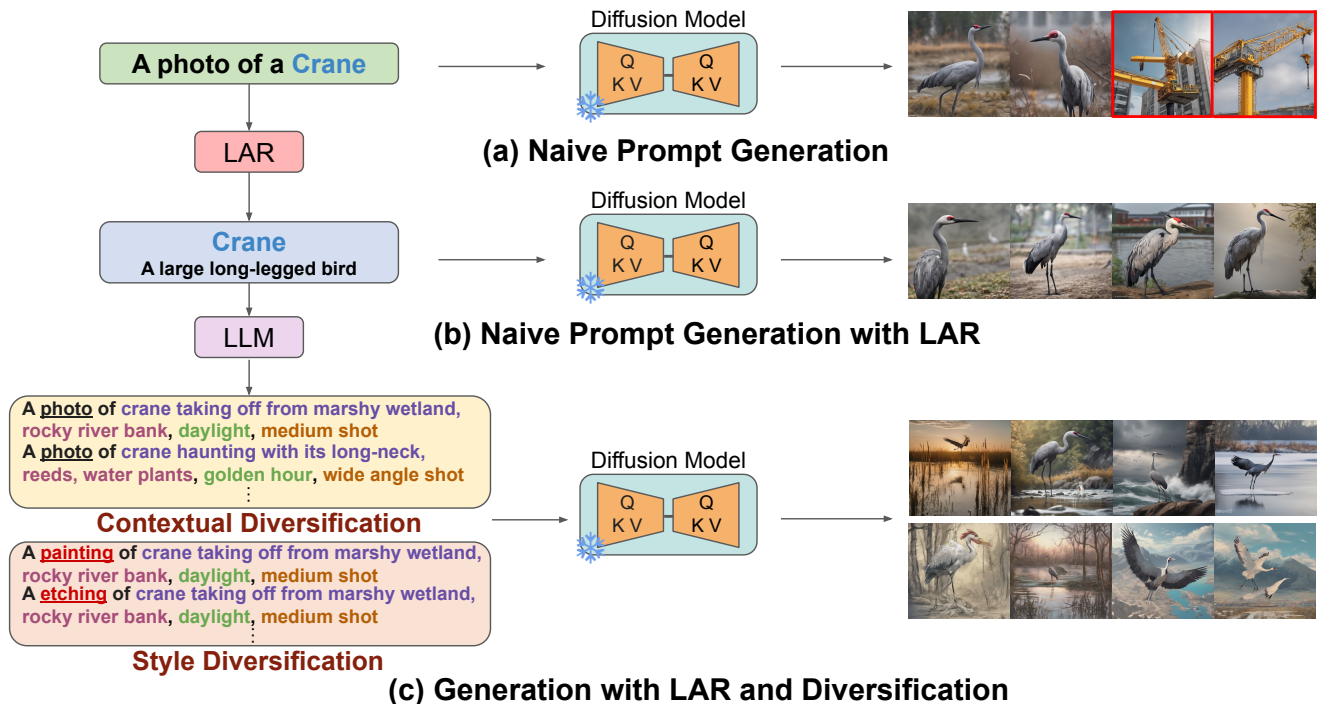


Figure 2. **Illustration of our synthetic data generation pipeline.** (a) Generating synthetic data with naive prompts can lead to incorrect semantics for classes with ambiguous names (e.g., the bird vs. the machine for “crane”). (b) Our Label Ambiguity Resolution (LAR) procedure resolves ambiguity in labels while preserving similar semantics in the generated images. (c) Our diversification procedure includes contextual diversification (CD) and style diversification (SD) by prompting an LLM to produce contextualized descriptions of images featuring class c (“crane” in this example) that combines different aspects (indicated by different colors in the figure): **foreground objects**, **background objects**, **lighting condition**, **camera angle**, and different **styles**.

24, 28, 36, 45]. With the recent introduction of large-scale image-text datasets [48, 49] and image-text foundation models like CLIP [36], state-of-the-art diffusion models [35, 42, 45, 46, 57] are able to perform text-to-image generation in an open-vocabulary manner. For example, the latent diffusion model (LDM) [45] conducts diffusion processes in the latent space; Imagen [46], on the other hand, directly runs diffusion steps at the pixel level. Recent works also extend these models for better control in image generation [3, 6, 25, 33, 58]. This paper’s focus is not to improve state-of-the-art diffusion models; instead, we propose a new framework that leverages such models to improve recognition model performance on large-scale datasets.

Improving Recognition Models with Synthetic Data.

We position our work within the line of work that studies how to improve visual recognition models with synthetic data from 3D-rendering [15, 22, 55, 59], simulation environments [11, 14, 16, 44], or generative models [1, 18, 20, 30, 31, 34]. Early work [1, 30, 31] typically trained a generative adversarial network [17] or its variant [5, 26, 27] on the target dataset to generate augmenting synthetic images. Recent work explores the potential of

synthetic images from diffusion models to improve image classification [20, 34, 47]. For example, [20, 29] shows that CLIP classification on a target dataset can be improved with synthetic data from diffusion models; Sariyildiz et al. [47] uses only synthetic data to train image classification models from scratch; Lin et al. [34] extends this study to object detection by pasting object-centric synthetic images onto training data under the few-shot scenario. Most related to our work, Azizi et al. [2] recently showed that synthetic data from Imagen [46] finetuned on ImageNet can improve recognition accuracy on ImageNet. Our work, on the other hand, follows a more practical setup: instead of training with only synthetic data or tuning specific pretrained models, we combine real images from ImageNet and synthetic images from off-the-shelf diffusion models (*i.e.*, no dataset specific finetuning) to maximize visual recognition performance. We demonstrate that with the refined data generation pipeline and proper training recipes, recognition models trained with our synthetic data show significant improvement over prior work that leverage finetuned generative models.

3. Approach

In this section, we introduce our framework from two main aspects: synthetic data generation and recognition model training. At a high level, we leverage a latest variant of an off-the-shelf latent diffusion model (LDM) [45] without any finetuning to generate our synthetic images, and train our recognition models using both real training images and generated synthetic images with a carefully designed training recipe.

3.1. Label Ambiguity Resolution

Real-world datasets, such as ImageNet [12], often present a challenge where class labels can carry multiple, sometimes divergent meanings. For instance, the term *crane* could refer to a type of construction machine or a species of bird. These dual interpretations lead to generations with significantly divergent semantics if not addressed properly: construction machine images are generated when the intended class refers to the bird. While existing solutions tackle this problem by leveraging dataset-specific hierarchical information [47] or involving manual processing [41], we propose a more comprehensive and, importantly, manual effort-free approach.

Our approach is centered around each class name c . Rather than manually curating a specific hierarchy for class names, we turn to LLMs for assistance. Given class c with N real training images, we query an LLM to extract K possible meaning phrases $\{P_i^c\}_{i=1}^K$ associated with c and compute their text embeddings $\{\phi(P_i^c)\}_{i=1}^K$ using the CLIP [41] text encoder ϕ . We also extract image embeddings $\{\theta(I_j^c)\}_{j=1}^N$ for the real training images $\{I_j^c\}_{j=1}^N$ using the CLIP visual encoder θ . We then compute the image-text similarities and select the meaning phrase with highest similarity \hat{P}^c :

$$\hat{P}^c = \arg \max_{P_i^c} \sum_{j=1}^N \theta(I_j^c) \cdot \phi(P_i^c) \quad (1)$$

This process helps pinpoint the most similar meaning \hat{P}^c which is then used as an additional textual description alongside class name c during synthetic data generation. By leveraging the power of LLMs and CLIP, we minimize manual effort and ensure that the synthetic data accurately represents the intended semantics even in situations where the class name has multiple meanings; see Fig. 2 (b).

3.2. Diversifying Synthetic Images

The process of diversifying synthetic images goes beyond a mere reliance on class names (c) and their associated meanings (\hat{P}^c). Although diffusion models preserve some level of diversity even for the same text input, we seek to achieve further diversification to improve the recognition

model. Specifically, our approach introduces two distinct methods for diversification: contextualized diversification (CD) and stylized diversification (SD), each founded on different principles and mechanisms.

Contextualized diversification (CD) is dedicated to producing photo-realistic synthetic images for each class c while maximizing diversity in their contexts. In CD, diversity is achieved through the incorporation of contextual foreground and background objects, which enrich the visual content of the synthetic images. Specifically, we prompt an LLM to produce contextualized descriptions of images featuring class c in a specific way that combines foreground objects, background objects, lighting condition, and camera angle. An example is shown as follows:

```
Imagine there is a photo of {class c}.
What foreground and background objects
can show up together with it? Describe
the photo in the following four aspects:
- Foreground
- Background
- Lighting Condition
- Camera Angle
```

We collect 600 responses from the LLM for each class and form the generation prompt by joining the descriptions from each aspect with a comma and with the prefix *a photograph of* to promote photo-realism.

Prompting an LLM in this way results in better responses than simply asking for a caption of a specific object class, as the LLM may return a generic description of the class name without much context.

The inclusion of these contextual elements not only provides a more nuanced and intricate description of the object class, but more importantly, it helps overcome any bias in the original dataset by incorporating knowledge from the LLM in generation.

Compared to finetuning diffusion models on the target dataset [2], our approach is able to generate synthetic images featuring the same class but containing contextual information beyond the original dataset, giving it potential to generalize better on out-of-distribution datasets (as we show in Section 4).

Stylized diversification (SD) is built on top of contextual diversification with an emphasis on generating synthetic images that exhibit a wide range of artistic styles. This approach goes beyond mere realism and delves into the realm of creative expression, allowing for a broader spectrum of synthetic images that cater to diverse aesthetic preferences. Specifically, we query an LLM for 60 different art styles (the list is provided in the Appendix) and replace the keyword “photograph” in the prompts from CD with each art style (e.g., change “a photograph of” to “a painting of”) to form the new generation prompts. In our implementation, we generate the same number of synthetic images using prompts from CD and SD; see Fig. 2 (c).

Again, since both CD and SD are realized with the help of an LLM, it not only automates the process to save human labor, but also ensures that the diversification of synthetic images is achieved in a consistent manner and at scale.

3.3. Mitigating Domain Shifts in Training

Although state-of-the-art diffusion models are capable of generating high-quality, photo-realistic synthetic images, the distribution gap remains between these synthetic images and their real counterparts. This divergence is most notably observed in the nearly separable features that characterize these images within the feature space [38].

As the scale of synthetic images grows, the risk of the recognition model overfitting on synthetic images also grows. Such overfitting can significantly undermine the recognition model’s performance, especially when synthetic images start to dominate the training data. As shown in prior work [2], the overall accuracy starts to drop when synthetic data outnumber real ones and it leads to -2.69% accuracy drop when synthetic data becomes 9x of real data. To circumvent this issue, we draw inspiration from the domain adaptation literature and view real and synthetic images as from two separate domains. This realization allows us to introduce auxiliary batch normalization layers [8, 32, 50] into the recognition model to separately process synthetic images from real ones. These additional BN layers play a pivotal role in bridging the domain gap as they prevent the batch statistics of synthetic data from disturbing the running means and variances for real images.

In addition, despite the potentially larger scale of synthetic images relative to real images, we enforce equal sampling weights for both the real and synthetic images during training so that each training batch roughly contains the same number of real and synthetic images. This avoids synthetic data from dominating each training batch and thus leading to domain overfitting. The loss we use to train the recognition model is:

$$\mathcal{L} = - \sum_{i=1}^{N_{\text{real}}} y_i \log(f(x_i)) - \lambda \cdot \sum_{j=1}^{N_{\text{synthetic}}} y_j \log(f'(x_j))$$

where f and f' denotes the model weights for real and synthetic images (i.e., they share weights except for BN layers) and λ is a tunable hyper-parameter which enables explicit control of the contribution of synthetic data in training.

4. Experiments

Datasets and Evaluation. We train our model using real images from ImageNet [12] and synthetic data generated with our pipeline. Each model is evaluated on ImageNet-val as the in-distribution evaluation. We further consider three ImageNet variations: ImageNet-V2 [43],

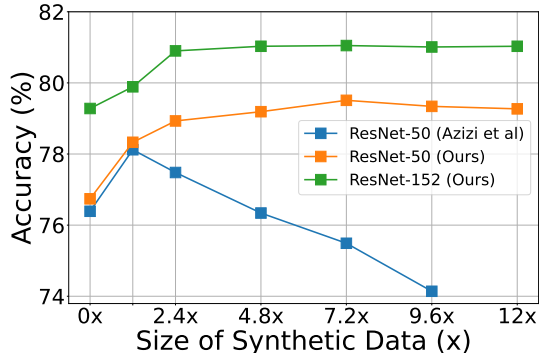


Figure 3. **Top-1 Accuracy as Synthetic Data Scales up.** In contrast to findings in previous work [2] (blue line), our method is able to scale up recognition training, with consistent accuracy improvement as the number of synthetic samples increases even after they outnumber the real samples.

ImageNet-Sketch [54], ImageNet-Rendition [21] to evaluate the out-of-distribution generalization capability of our models. Specifically, ImageNet-V2 is a reproduced version of ImageNet classes with distribution shifts; ImageNet-Sketch and -Rendition contains sketch and rendition versions of ImageNet classes, respectively.

Model Architectures. Following prior work [2], we evaluate our approach using different convolutional neural networks (CNNs) and vision transformer architectures. We consider ResNet-{50, 101, 152} [19] for CNNs and DeiT-{S, B, L} [52] for vision transformers.

Implementation Details. We use *gpt-3.5-turbo*, an improved version of InstructGPT [39] and GPT-3 [7] from OpenAI as our LLM for contextual diversification and style diversification. For each class, we prompt the LLM to generate 600 contextual-diversified prompts and 60 style keywords to form style-diversified prompts in synthetic data generation. We use the latest variation of LDM [45] to generate our synthetic data. All synthetic images are generated with size of 1024x1024 and downsampled to 256x256 for efficient storage and higher throughput in data loading. When training recognition models, we closely follow the training setup from prior work [2]. Specifically, we train ResNet models for 130 epochs and all vision transformer variants for 300 epochs. We set the synthetic loss weight λ to 0.6 for all experiments, which is selected based on in-domain evaluation of ResNet-50 alone. For full details of our hyper-parameters, please refer to our Appendix.

4.1. Scaling-up Training with Synthetic Data

We first demonstrate how the performances change as we scale up the size of synthetic data from 1.2M to 12M. Since ImageNet has roughly 1.2M real training images, our selected range of synthetic data sizes increases from 1x Im-

	<u>IMAGENET-VAL</u>				IMAGENET-V2			IMAGENET-S			IMAGENET-R		
	Real Only	Azizi et al [2]	Ours	Δ	Real Only	Ours	Δ	Real Only	Ours	Δ	Real Only	Ours	Δ
ResNet-50	76.74	78.17	79.27	+2.53	72.20	75.09	+2.89	25.01	32.56	+7.55	24.55	30.32	+5.77
ResNet-101	79.01	79.74	80.76	+1.75	74.75	76.89	+2.14	27.92	33.32	+5.40	27.08	31.22	+4.14
ResNet-152	79.28	80.15	81.05	+1.77	75.11	77.32	+2.21	29.98	33.62	+3.64	28.29	32.45	+4.16
DeiT-S	78.97	80.49	81.32	+2.35	74.66	77.61	+2.95	28.49	42.29	+13.80	27.93	39.68	+11.75
DeiT-B	81.79	82.84	82.99	+1.20	77.35	79.16	+1.81	36.31	47.65	+11.34	34.47	44.14	+9.67
DeiT-L	82.22	83.05	83.53	+1.31	78.82	79.45	+0.63	39.90	50.01	+10.11	37.21	46.48	+9.47

Table 1. **Top-1 Accuracy on ImageNet and out-of-domain variations.** We train each model with real ImageNet training images and synthetic images generated with our pipeline. In-domain evaluation is conducted on ImageNet-val (underlined) and out-of-domain evaluations are conducted on ImageNet-V2, ImageNet-Sketch and ImageNet-Rendition. Specifically, we apply the same model trained with ImageNet real and our synthetic images on these out-of-domain evaluation datasets without further finetuning for evaluation. Δ denotes the margin of improvement of our approach over baseline models trained with real images only.

ageNet scale to 10x ImageNet scale. We use the same amount of synthetic images from contextual diversification and style diversification for our models.

Results are presented in Figure 3. In prior work [2], ResNet-50 suffers performance degradation as the size of synthetic data increases: the accuracy becomes even worse than the baseline trained with only real images when synthetic data exceeds 4x ImageNet scale (4.8M). In stark contrast, models trained with our approach demonstrate consistent improvement up to 6x synthetic images at ImageNet scale. Also unlike [2] which observed significant performance degradation when further scaling up the synthetic images, our approach produces consistent model quality even beyond the point of saturation. This is important as it demonstrates the untapped potential for practical use of synthetic data at a large scale.

4.2. Main Results

We next present the evaluation results of our approach on ImageNet. In Table 1, we report results of training with ImageNet real images and our diversified synthetic images for each architecture.

When evaluating on ImageNet-val, our approach demonstrates significant and consistent improvement over both the baseline model trained with only real data, and the prior state-of-the-art that uses an ImageNet finetuned diffusion model to generate synthetic data [2]. For example, our approach achieves +2.53% and +1.10% absolute accuracy improvement over the real image baseline and prior approach [2] with ResNet-50, respectively. With larger CNN models like ResNet-101 and ResNet-152, our approach also achieves remarkable improvement (1.02% and 0.90% respectively) over prior work [2]. For vision transformer variants like DeiT-{B, L}, which already demonstrate strong performance on ImageNet, our method can still further improve their performance. These results validate the benefit of our framework in leveraging synthetic data at a large scale across model architectures.

Furthermore, our method shows strong performance

on out-of-distribution generalization. When evaluated on ImageNet-V2, ImageNet-Sketch, and ImageNet-Rendition, our method generally achieves +3% to +7% accuracy improvement over the real-only CNN models. With vision transformers, the improvement is even more significant: DeiT-B trained with our diversified synthetic data achieves 11.34% and 9.67% accuracy improvement on ImageNet-Sketch and ImageNet-Rendition over the real baseline. Our results prove the efficacy of diversified synthetic data to improve both in-domain and out-of-domain generalization.

4.3. Results for Low-data and Long-tail Settings

Evaluation on Low-data Regime. We demonstrate the effectiveness of our method in settings where only limited real training images are available. Specifically, we sample {100, 200, 500} real training images per class to form the real training data and use 2x additional synthetic data of ImageNet scale (2.4M) from our pipeline. We train each recognition model for 100 epochs as models usually converge faster under the low-data regime.

As shown in Table 3, our improvements on ImageNet transfer well to the low-data regime where only limited real images are available. When training with 100 real images per class, additional 2x synthetic data usually brings +10% accuracy improvement. With 500 real images per class, our model achieves 74.87% and 75.63% for ResNet-101 and ResNet-152, which largely closes the gap to training with full ImageNet images (79.01% for ResNet-101 and 79.28% for ResNet-152). These results show that leveraging diversified synthetic data can significantly reduce annotation effort (*e.g.*, 2x) with minor performance degradation.

Evaluation under long-tail distribution. We also show our pipeline enables strong improvements when the real images follow a long-tailed distribution. For comprehensive evaluation under different imbalance ratios, we randomly sample a long-tailed distribution with imbalance ratio γ in {50, 100, 200} from the original ImageNet training data, following an exponential imbalance function [10]. Specif-

	Training Data	$\gamma = 50$			$\gamma = 100$			$\gamma = 200$		
		Many-shot	Medium-shot	Few-shot	Many-shot	Medium-shot	Few-shot	Many-shot	Medium-shot	Few-shot
ResNet-50	Real	78.63	69.08	45.69	79.02	68.12	39.35	78.99	66.58	33.31
ResNet-50	Real + 2x Syn	82.19	72.43	51.18	81.36	71.35	45.56	81.61	69.78	39.74
ResNet-152	Real	80.60	72.09	49.19	80.77	70.25	42.81	80.95	68.72	36.26
ResNet-152	Real + 2x Syn	82.96	75.51	54.50	83.28	74.48	49.12	83.29	72.88	43.52

Table 2. **Evaluation of Long-tail Distribution for Real Images.** We evaluate each model with an imbalance ratio γ in $\{50, 100, 200\}$ by subsampling ImageNet real training images and using 2x additional synthetic data of original ImageNet scale (2.4M) from our pipeline to train the models. Compared to the baseline trained with real images, our approach shows consistent performance improvements, especially on few-shot classes.

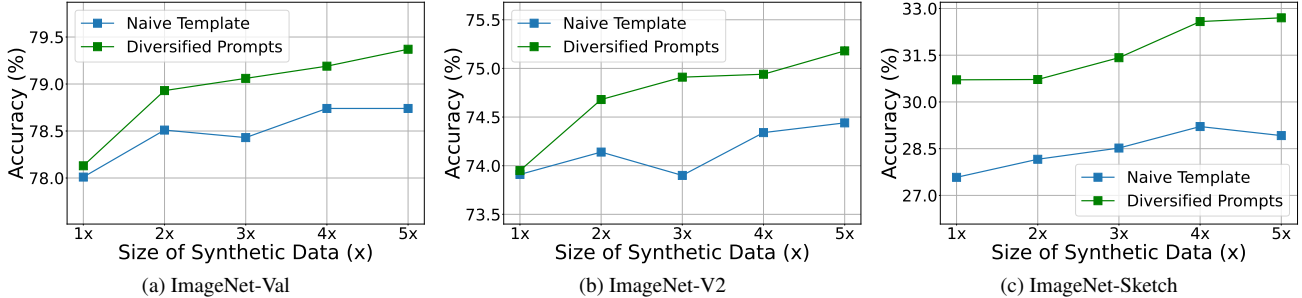


Figure 4. **Naive vs. Diversified Prompts.** As the synthetic images increase from 1.2M to 6M, we observe a consistent improvement from diversification of synthetic data, and such improvement becomes more distinct as the scale of synthetic data increases. This trend is consistent across different evaluation sets.

	Training Data	N=100	N=200	N=500
ResNet50	Real Only	47.83	58.76	68.04
ResNet50	Real + 2x Syn	60.95	65.19	73.11
ResNet101	Real Only	48.09	59.64	69.25
ResNet101	Real + 2x Syn	62.01	67.39	74.87
ResNet152	Real Only	48.05	60.33	70.91
ResNet152	Real + 2x Syn	63.53	69.05	75.63

Table 3. **Low-data Regime Evaluation.** Our models demonstrate consistent improvement over models trained with only real images.

	ResNet-50	ResNet-101	ResNet-152
Vanilla BN	78.32	79.92	80.43
Separate BN	78.93	80.34	81.05

Table 4. **Vanilla vs. Separate BN.** Results are generated with 2.4M synthetic images with diversification. Separate BN is demonstrated to be effective for training on real+synthetic data, across various model architectures.

ically, the number of real images for class k is computed as $n_k = n_1 \cdot \gamma^{-(k-1)/(K-1)}$, where K is the total number of classes. n_1 is the number of labels for the most frequent class and is set to 1300, which is the max number of images per class on ImageNet. Evaluation is conducted on

ImageNet-val, which is roughly balanced. We report the accuracy for many-shot classes, medium-shot classes, and few-shot classes. Results are shown in Table 2 and models trained with our synthetic data consistently outperform the real-only models over many-shot, medium-shot and few-shot classes. For few-shot classes, our approach can even improve by 5% to 7% accuracy, which demonstrates the efficacy of diversified synthetic data to tackle long-tail problems.

4.4. Ablation Studies

We next present ablation studies. Unless otherwise noted, all experiments in this section are conducted with 2x (2.4M) synthetic images generated with contextual and style diversification.

Importance of Diversifying Synthetic Images. Figure 4 compares the performance of a ResNet-50 model on ImageNet-val, ImageNet-V2, and ImageNet-Sketch when trained with different amounts of synthetic data generated with naive prompts *A photo of {c}* and our diversified prompts described in Section 3.2. We apply separate BN to train both models for fair comparison. As we increase the size of synthetic images from 1.2M to 6M, we see a consistent improvement from diversified synthetic images on ImageNet-val, ImageNet-V2, and ImageNet-Sketch. The improvement is more significant as the scale of synthetic data increases, which demonstrates the critical role that di-

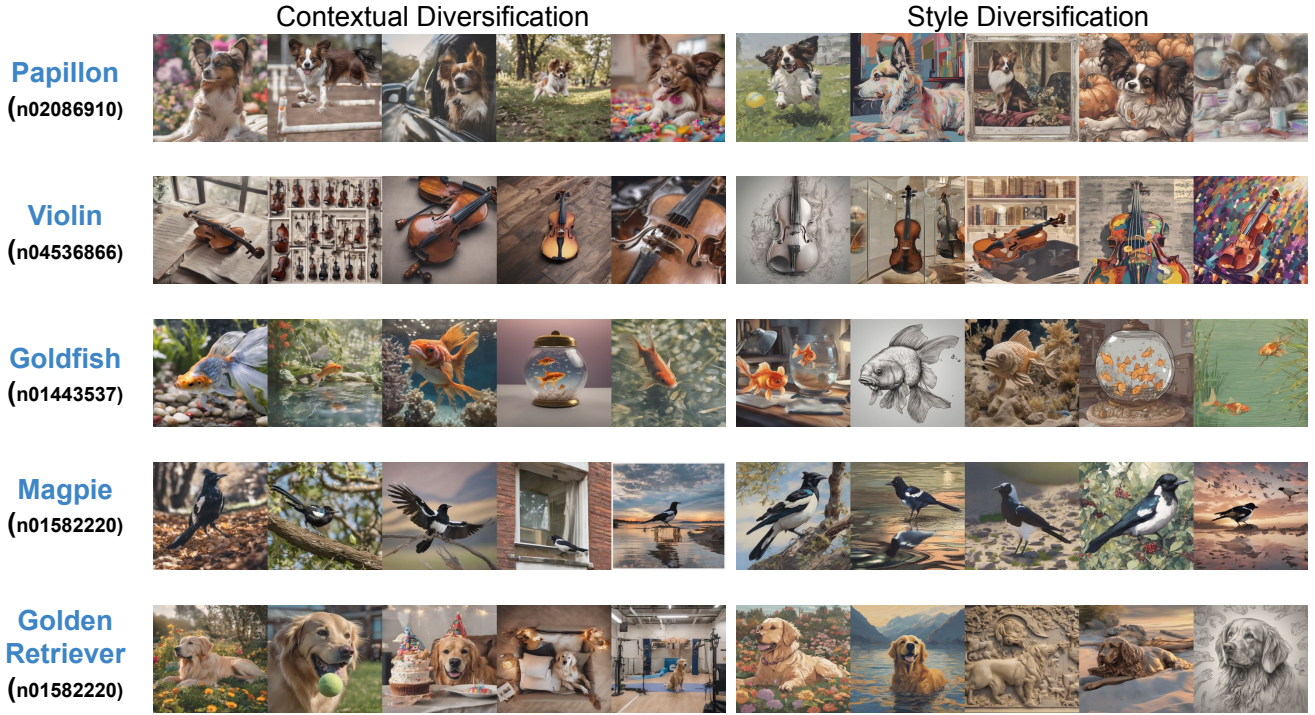


Figure 5. **Example Generations.** We show example synthetic images from our approach. Within the same class, contextual diversification creates diverse synthetic images by introducing varying contextual elements, lighting conditions, and camera angles. In contrast, style diversification alters the visual style of synthetic images. We provide example diversified prompts in Appendix for reference.

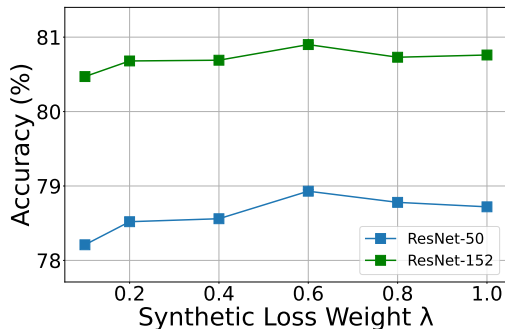


Figure 6. **Sensitivity to Synthetic Loss Weights λ .** As shown in the plot, our approach is robust to λ in a wide value range (*i.e.*, in $[0.2, 1.0]$).

versifying synthetic images plays in our framework.

Importance of Separate BN in CNNs. Using separate batch norm layers (BN) for real and synthetic images is a critical design in our framework and we demonstrate its importance in Table 4. Using separate BN significantly and consistently improves performance for different ResNet architectures, which validates the importance of this design.

Sensitivity to Synthetic Loss Weights. Since we introduce a tunable hyper-parameter λ in our framework to con-

trol the overall contribution of synthetic data in training, we demonstrate how sensitive our approach is with respect to λ . As shown in Figure 6, the accuracy of ResNet-50 and ResNet-152 is not affected much by the choice of λ unless its value becomes very small (*e.g.*, $\lambda < 0.2$). Therefore, we simply select the best-performing value $\lambda = 0.6$ on ResNet-50 for all our experiments.

Visualization of Synthetic Images. We present example synthetic images used in our experiments. As shown in Figure 5, our diversification approach achieves significant levels of diversification through contextual diversification (CD) and style diversification (SD). For the same class, contextual diversification introduces diversity into synthetic images by incorporating different contextual objects, varied lighting conditions, and altered camera angles. In contrast, style diversification focuses on modifying the visual style of synthetic images.

5. Conclusion

We presented a scalable framework to leverage an off-the-shelf diffusion model to generate large-scale synthetic datasets that help improve visual recognition models. We demonstrated that with our methods on label ambiguity resolution, contextual and style prompt diversification, and

training strategies to mitigate the real/synthetic domain gap, recognition models trained with our framework significantly outperforms prior work that requires finetuning of diffusion models on target datasets. Furthermore, we also demonstrated that models trained with our framework show strong out-of-distribution generalization performance and better ability to transfer to downstream tasks compared to previous methods. We hope our work can inspire future research on leveraging synthetic data to improve recognition models.

Acknowledgments

This work was supported in part by NSF CAREER IIS2150012, and Institute of Information & communications Technology Planning & Evaluation(IITP) grant funded by the Korea government(MSIT) (No. RS2022-00187238, Development of Large Korean Language Model Technology for Efficient Pre-training).

References

- [1] Adamu Ali-Gombe, Eyad Elyan, Yann Savoye, and Chrisina Jayne. Few-shot classifier gan. In *2018 International Joint Conference on Neural Networks (IJCNN)*, pages 1–8. IEEE, 2018. [3](#)
- [2] Shekoofeh Azizi, Simon Kornblith, Chitwan Saharia, Mohammad Norouzi, and David J Fleet. Synthetic data from diffusion models improves imagenet classification. *arXiv preprint arXiv:2304.08466*, 2023. [1](#), [2](#), [3](#), [4](#), [5](#), [6](#)
- [3] Omer Bar-Tal, Lior Yariv, Yaron Lipman, and Tali Dekel. Multidiffusion: Fusing diffusion paths for controlled image generation. 2023. [3](#)
- [4] Lukas Bossard, Matthieu Guillaumin, and Luc Van Gool. Food-101—mining discriminative components with random forests. In *Computer Vision—ECCV 2014: 13th European Conference, Zurich, Switzerland, September 6–12, 2014, Proceedings, Part VI 13*, pages 446–461. Springer, 2014. [3](#)
- [5] Andrew Brock, Jeff Donahue, and Karen Simonyan. Large scale gan training for high fidelity natural image synthesis. *arXiv preprint arXiv:1809.11096*, 2018. [3](#)
- [6] Tim Brooks, Aleksander Holynski, and Alexei A Efros. Instructpix2pix: Learning to follow image editing instructions. In *Proceedings of the IEEE/CVF Conference on Computer Vision and Pattern Recognition*, pages 18392–18402, 2023. [3](#)
- [7] Tom Brown, Benjamin Mann, Nick Ryder, Melanie Subbiah, Jared D Kaplan, Prafulla Dhariwal, Arvind Neelakantan, Pranav Shyam, Girish Sastry, Amanda Askell, et al. Language models are few-shot learners. *Advances in neural information processing systems*, 33:1877–1901, 2020. [5](#)
- [8] Woong-Gi Chang, Tackgeun You, Seonguk Seo, Suha Kwak, and Bohyung Han. Domain-specific batch normalization for unsupervised domain adaptation. In *Proceedings of the IEEE/CVF conference on Computer Vision and Pattern Recognition*, pages 7354–7362, 2019. [2](#), [5](#)
- [9] M. Cimpoi, S. Maji, I. Kokkinos, S. Mohamed, , and A. Vedaldi. Describing textures in the wild. In *Proceedings of the IEEE Conf. on Computer Vision and Pattern Recognition (CVPR)*, 2014. [3](#)
- [10] Yin Cui, Menglin Jia, Tsung-Yi Lin, Yang Song, and Serge Belongie. Class-balanced loss based on effective number of samples. In *Proceedings of the IEEE/CVF conference on computer vision and pattern recognition*, pages 9268–9277, 2019. [6](#), [2](#)
- [11] Celso M de Melo, Antonio Torralba, Leonidas Guibas, James DiCarlo, Rama Chellappa, and Jessica Hodgins. Next-generation deep learning based on simulators and synthetic data. *Trends in cognitive sciences*, 2022. [3](#)
- [12] Jia Deng, Wei Dong, Richard Socher, Li-Jia Li, Kai Li, and Li Fei-Fei. Imagenet: A large-scale hierarchical image database. In *2009 IEEE conference on computer vision and pattern recognition*, pages 248–255. Ieee, 2009. [1](#), [4](#), [5](#)
- [13] Prafulla Dhariwal and Alexander Nichol. Diffusion models beat gans on image synthesis. *Advances in neural information processing systems*, 34:8780–8794, 2021. [1](#), [2](#)
- [14] Alexey Dosovitskiy, German Ros, Felipe Codevilla, Antonio Lopez, and Vladlen Koltun. Carla: An open urban driving simulator. In *Conference on robot learning*, pages 1–16. PMLR, 2017. [3](#)
- [15] Gang Fu, Qing Zhang, Lei Zhu, Chunxia Xiao, and Ping Li. Towards high-quality specular highlight removal by leveraging large-scale synthetic data. In *Proceedings of the IEEE/CVF International Conference on Computer Vision*, pages 12857–12865, 2023. [3](#)
- [16] Chuhan Gan, Jeremy Schwartz, Seth Alter, Damian Mrowca, Martin Schrimpf, James Traer, Julian De Freitas, Jonas Kubilius, Abhishek Bhandwaldar, Nick Haber, et al. Threed-world: A platform for interactive multi-modal physical simulation. *arXiv preprint arXiv:2007.04954*, 2020. [3](#)
- [17] Ian Goodfellow, Jean Pouget-Abadie, Mehdi Mirza, Bing Xu, David Warde-Farley, Sherjil Ozair, Aaron Courville, and Yoshua Bengio. Generative adversarial nets. *Advances in neural information processing systems*, 27, 2014. [3](#)
- [18] Sven Gowal, Sylvester-Alvise Rebuffi, Olivia Wiles, Florian Stimberg, Dan Andrei Calian, and Timothy A Mann. Improving robustness using generated data. *Advances in Neural Information Processing Systems*, 34:4218–4233, 2021. [3](#)
- [19] Kaiming He, Xiangyu Zhang, Shaoqing Ren, and Jian Sun. Deep residual learning for image recognition. In *Proceedings of the IEEE conference on computer vision and pattern recognition*, pages 770–778, 2016. [5](#)
- [20] Ruifei He, Shuyang Sun, Xin Yu, Chuhui Xue, Wenqing Zhang, Philip Torr, Song Bai, and Xiaojuan Qi. Is synthetic data from generative models ready for image recognition? *arXiv preprint arXiv:2210.07574*, 2022. [1](#), [3](#)
- [21] Dan Hendrycks, Steven Basart, Norman Mu, Saurav Kadavath, Frank Wang, Evan Dorundo, Rahul Desai, Tyler Zhu, Samyak Parajuli, Mike Guo, Dawn Song, Jacob Steinhardt, and Justin Gilmer. The many faces of robustness: A critical analysis of out-of-distribution generalization. *ICCV*, 2021. [2](#), [5](#)
- [22] Robin Hesse, Simone Schaub-Meyer, and Stefan Roth. Funnybirds: A synthetic vision dataset for a part-based analysis

- of explainable ai methods. In *Proceedings of the IEEE/CVF International Conference on Computer Vision*, pages 3981–3991, 2023. 3
- [23] Jonathan Ho, Ajay Jain, and Pieter Abbeel. Denoising diffusion probabilistic models. *Advances in neural information processing systems*, 33:6840–6851, 2020. 1
- [24] Jonathan Ho, Chitwan Saharia, William Chan, David J Fleet, Mohammad Norouzi, and Tim Salimans. Cascaded diffusion models for high fidelity image generation. *The Journal of Machine Learning Research*, 23(1):2249–2281, 2022. 1, 3
- [25] Lianghua Huang, Di Chen, Yu Liu, Yujun Shen, Deli Zhao, and Jingren Zhou. Composer: Creative and controllable image synthesis with composable conditions. *arXiv preprint arXiv:2302.09778*, 2023. 3
- [26] Tero Karras, Samuli Laine, and Timo Aila. A style-based generator architecture for generative adversarial networks. In *Proceedings of the IEEE/CVF conference on computer vision and pattern recognition*, pages 4401–4410, 2019. 3
- [27] Tero Karras, Samuli Laine, Miika Aittala, Janne Hellsten, Jaakko Lehtinen, and Timo Aila. Analyzing and improving the image quality of stylegan. In *Proceedings of the IEEE/CVF conference on computer vision and pattern recognition*, pages 8110–8119, 2020. 3
- [28] Diederik Kingma, Tim Salimans, Ben Poole, and Jonathan Ho. Variational diffusion models. *Advances in neural information processing systems*, 34:21696–21707, 2021. 3
- [29] Bo Li, Haotian Liu, Liangyu Chen, Yong Jae Lee, Chunyuan Li, and Ziwei Liu. Benchmarking and analyzing generative data for visual recognition. *arXiv preprint arXiv:2307.13697*, 2023. 3
- [30] Daiqing Li, Junlin Yang, Karsten Kreis, Antonio Torralba, and Sanja Fidler. Semantic segmentation with generative models: Semi-supervised learning and strong out-of-domain generalization. In *Proceedings of the IEEE/CVF Conference on Computer Vision and Pattern Recognition*, pages 8300–8311, 2021. 3
- [31] Daiqing Li, Huan Ling, Seung Wook Kim, Karsten Kreis, Sanja Fidler, and Antonio Torralba. Bigdatasetgan: Synthesizing imagenet with pixel-wise annotations. In *Proceedings of the IEEE/CVF Conference on Computer Vision and Pattern Recognition*, pages 21330–21340, 2022. 3
- [32] Yanghao Li, Naiyan Wang, Jianping Shi, Xiaodi Hou, and Jiaying Liu. Adaptive batch normalization for practical domain adaptation. *Pattern Recognition*, 80:109–117, 2018. 2, 5
- [33] Yuheng Li, Haotian Liu, Qingyang Wu, Fangzhou Mu, Jianwei Yang, Jianfeng Gao, Chunyuan Li, and Yong Jae Lee. Gligen: Open-set grounded text-to-image generation. In *Proceedings of the IEEE/CVF Conference on Computer Vision and Pattern Recognition*, pages 22511–22521, 2023. 3
- [34] Shaobo Lin, Kun Wang, Xingyu Zeng, and Rui Zhao. Explore the power of synthetic data on few-shot object detection. In *Proceedings of the IEEE/CVF Conference on Computer Vision and Pattern Recognition*, pages 638–647, 2023. 3
- [35] Alex Nichol, Prafulla Dhariwal, Aditya Ramesh, Pranav Shyam, Pamela Mishkin, Bob McGrew, Ilya Sutskever, and Mark Chen. Glide: Towards photorealistic image generation and editing with text-guided diffusion models. *arXiv preprint arXiv:2112.10741*, 2021. 1, 3
- [36] Alexander Quinn Nichol and Prafulla Dhariwal. Improved denoising diffusion probabilistic models. In *International Conference on Machine Learning*, pages 8162–8171. PMLR, 2021. 1, 3
- [37] Maria-Elena Nilsback and Andrew Zisserman. Automated flower classification over a large number of classes. In *2008 Sixth Indian conference on computer vision, graphics & image processing*, pages 722–729. IEEE, 2008. 3
- [38] Utkarsh Ojha, Yuheng Li, and Yong Jae Lee. Towards universal fake image detectors that generalize across generative models. In *Proceedings of the IEEE/CVF Conference on Computer Vision and Pattern Recognition*, pages 24480–24489, 2023. 2, 5
- [39] Long Ouyang, Jeffrey Wu, Xu Jiang, Diogo Almeida, Carroll Wainwright, Pamela Mishkin, Chong Zhang, Sandhini Agarwal, Katarina Slama, Alex Ray, et al. Training language models to follow instructions with human feedback. *Advances in Neural Information Processing Systems*, 35: 27730–27744, 2022. 5
- [40] Omkar M Parkhi, Andrea Vedaldi, Andrew Zisserman, and CV Jawahar. Cats and dogs. In *2012 IEEE conference on computer vision and pattern recognition*, pages 3498–3505. IEEE, 2012. 3
- [41] Alec Radford, Jong Wook Kim, Chris Hallacy, Aditya Ramesh, Gabriel Goh, Sandhini Agarwal, Girish Sastry, Amanda Askell, Pamela Mishkin, Jack Clark, et al. Learning transferable visual models from natural language supervision. In *International conference on machine learning*, pages 8748–8763. PMLR, 2021. 1, 2, 4
- [42] Aditya Ramesh, Prafulla Dhariwal, Alex Nichol, Casey Chu, and Mark Chen. Hierarchical text-conditional image generation with clip latents, 2022. URL <https://arxiv.org/abs/2204.06125>, 7, 2022. 1, 3
- [43] Benjamin Recht, Rebecca Roelofs, Ludwig Schmidt, and Vaishaal Shankar. Do imagenet classifiers generalize to imagenet? In *International conference on machine learning*, pages 5389–5400. PMLR, 2019. 2, 5
- [44] Stephan R Richter, Vibhav Vineet, Stefan Roth, and Vladlen Koltun. Playing for data: Ground truth from computer games. In *Computer Vision—ECCV 2016: 14th European Conference, Amsterdam, The Netherlands, October 11–14, 2016, Proceedings, Part II 14*, pages 102–118. Springer, 2016. 3
- [45] Robin Rombach, Andreas Blattmann, Dominik Lorenz, Patrick Esser, and Björn Ommer. High-resolution image synthesis with latent diffusion models. In *Proceedings of the IEEE/CVF conference on computer vision and pattern recognition*, pages 10684–10695, 2022. 1, 3, 4, 5
- [46] Chitwan Saharia, William Chan, Saurabh Saxena, Lala Li, Jay Whang, Emily L Denton, Kamyar Ghasemipour, Raphael Gontijo Lopes, Burcu Karagol Ayan, Tim Salimans, et al. Photorealistic text-to-image diffusion models with deep language understanding. *Advances in Neural Information Processing Systems*, 35:36479–36494, 2022. 1, 3

- [47] Mert Bulent Sariyildiz, Karteek Alahari, Diane Larlus, and Yannis Kalantidis. Fake it till you make it: Learning transferable representations from synthetic imagenet clones. In *CVPR 2023—IEEE/CVF Conference on Computer Vision and Pattern Recognition*, 2023. 1, 2, 3, 4
- [48] Christoph Schuhmann, Richard Vencu, Romain Beaumont, Robert Kaczmarczyk, Clayton Mullis, Aarush Katta, Theo Coombes, Jenia Jitsev, and Aran Komatsuzaki. Laion-400m: Open dataset of clip-filtered 400 million image-text pairs. *arXiv preprint arXiv:2111.02114*, 2021. 1, 3
- [49] Christoph Schuhmann, Romain Beaumont, Richard Vencu, Cade Gordon, Ross Wightman, Mehdi Cherti, Theo Coombes, Aarush Katta, Clayton Mullis, Mitchell Wortsman, et al. Laion-5b: An open large-scale dataset for training next generation image-text models. *Advances in Neural Information Processing Systems*, 35:25278–25294, 2022. 1, 3
- [50] Seonguk Seo, Yumin Suh, Dongwan Kim, Geeho Kim, Jongwoo Han, and Bohyung Han. Learning to optimize domain specific normalization for domain generalization. In *Computer Vision—ECCV 2020: 16th European Conference, Glasgow, UK, August 23–28, 2020, Proceedings, Part XXII 16*, pages 68–83. Springer, 2020. 2, 5
- [51] Jascha Sohl-Dickstein, Eric Weiss, Niru Maheswaranathan, and Surya Ganguli. Deep unsupervised learning using nonequilibrium thermodynamics. In *International conference on machine learning*, pages 2256–2265. PMLR, 2015. 2
- [52] Hugo Touvron, Matthieu Cord, Matthijs Douze, Francisco Massa, Alexandre Sablayrolles, and Hervé Jégou. Training data-efficient image transformers & distillation through attention. In *International conference on machine learning*, pages 10347–10357. PMLR, 2021. 5, 1
- [53] Hugo Touvron, Matthieu Cord, and Hervé Jégou. Deit iii: Revenge of the vit. In *European Conference on Computer Vision*, pages 516–533. Springer, 2022. 1
- [54] Haohan Wang, Songwei Ge, Zachary Lipton, and Eric P Xing. Learning robust global representations by penalizing local predictive power. In *Advances in Neural Information Processing Systems*, pages 10506–10518, 2019. 2, 5
- [55] Zhitao Yang, Zhongang Cai, Haiyi Mei, Shuai Liu, Zhaoxi Chen, Weiye Xiao, Yukun Wei, Zhongfei Qing, Chen Wei, Bo Dai, et al. Synbody: Synthetic dataset with layered human models for 3d human perception and modeling. *arXiv preprint arXiv:2303.17368*, 2023. 3
- [56] Yang You, Igor Gitman, and Boris Ginsburg. Scaling sgd batch size to 32k for imagenet training. *arXiv preprint arXiv:1708.03888*, 6(12):6, 2017. 1
- [57] Lili Yu, Bowen Shi, Ramakanth Pasunuru, Benjamin Muller, Olga Golovneva, Tianlu Wang, Arun Babu, Binh Tang, Brian Karrer, Shelly Sheynin, et al. Scaling autoregressive multi-modal models: Pretraining and instruction tuning. *arXiv preprint arXiv:2309.02591*, 2023. 1, 3
- [58] Lvmin Zhang, Anyi Rao, and Maneesh Agrawala. Adding conditional control to text-to-image diffusion models. In *Proceedings of the IEEE/CVF International Conference on Computer Vision*, pages 3836–3847, 2023. 3
- [59] Yang Zheng, Adam W Harley, Bokui Shen, Gordon Wetzstein, and Leonidas J Guibas. Pointodyssey: A large-scale synthetic dataset for long-term point tracking. In *Proceedings of the IEEE/CVF International Conference on Computer Vision*, pages 19855–19865, 2023. 3

Diversify, Don't Fine-Tune: Scaling Up Visual Recognition Training with Synthetic Images

Supplementary Material

A. Training Details

We describe the training details of our main experiments in this section (shown in Table 1). For training ResNet models, we keep most hyper-parameters the same as prior work [2] except for batch size and learning rate. Azizi et al [2] uses batch size 4096 and learning rate 1.6 and we double them in our experiments to expedite training. Echoing findings in previous work [56], we found this difference only makes training faster without much impact on model accuracy. Also, unlike [2] in which models are trained for 200 epochs, we train all models for 130 epochs, as we did not observe performance improvements by training them longer. Details can be found in Table A.

Model Parameter	ResNet-{50, 101, 152}
Epochs	130
Batch size	8192
Optimizer	Momentum
Learning rate	3.2
Decay method	Cosine
Weight decay	1e-4
Warmup epochs	5
Label smoothing	0.1
Dropout rate	0.25
Data Augment	RandAug

Table A. Training Details of ResNet Models.

When training large vision-transformer such as DeiT-B and DeiT-L [52], we have encountered numerical stability issue[†] when using the learning rate schedule from Azizi et al [2, 52]. Therefore, we follow the refined training setup [53] with the same number of epochs from prior work [2, 52]. The baseline model with real images trained with this new schedule achieves 81.28% top-1 accuracy for DeiT-B, which is slightly lower than the baseline from prior work [2]. Note that we use the same recipe for both the real-image baselines as well as for our method. Details can be found in Table B.

We use 6x synthetic data of ImageNet scale (7.2M) for ResNet models and DeiT-S and 2x (2.4M) for DeiT-B and DeiT-L. We attribute such difference to two reasons. First, larger vision transformer models generally take longer to

[†]Such difficulty is widely observed by other community users: <https://github.com/facebookresearch/deit/issues/29>

Model	DeiT-S	DeiT-B	DeiT-L
Epochs	300	300	300
Input Size	224	192	192
Batch size	4096	2048	2048
Optimizer	AdamW	Lamb	Lamb
Learning rate	0.004	0.003	0.003
Learning rate decay	Cosine	Cosine	Cosine
Weight decay	0.05	0.05	0.05
Warmup epochs	5	5	5
Label dsmoothing	0.1	0.1	0.1
Drop Path	0.1	0.2	0.45
Rand Augment	9	9	9
Mixup prob.	0.8	0.8	0.8
Cutmix prob.	1.0	1.0	1.0
Eval Crop Ratio	0.875	1.0	1.0

Table B. Training Details of Vision Transformer Models: DeiT-S [52], DeiT-B [52], and DeiT-L [52].

train per iteration. Second, those models are more sensitive to larger learning rates and linearly scaling up learning rate with batch sizes usually cause numeric stability issues. These two reasons together make training larger vision transformer models with more synthetic data take much longer than smaller models (more than a week in our infrastructure with 4 8-A100 GPU nodes). Therefore, we only use 2.4M synthetic data to train those larger models and significant improvement is already observed in Table 1.

B. Low-data and Long-tail Training

As shown in Table 2 and Table 3, diversified synthetic data from our approach can also improve model training under low-data regime and long-tail distribution of real images. We provide training details of these experiments in this section. These set of experiments are evaluated with ResNet architectures.

For low-data regime, we sample 100, 200, and 500 real images per class from ImageNet real images to construct low-data training set. For models trained with our synthetic data, we keep most the training settings same as Table A, which is used for ImageNet training except that we use 100 epochs as model usually converge faster under these conditions. For baseline models trained with real images, we use batch size 2048 and learning rate 0.88 to train these models as we found larger batch sizes produce significantly worse results for these models due to data scarcity.

	Training Data	$\gamma = 50$	$\gamma = 100$	$\gamma = 200$
ResNet-50	Real	64.65	62.06	59.48
ResNet-50	Real + 2x Syn	68.55	66.07	63.73
ResNet-152	Real	67.66	64.91	62.19
ResNet-152	Real + 2x Syn	70.81	68.70	66.31

Table C. **Evaluation of Long-tail Distribution for Real Images.** We evaluate each model with imbalance ratio γ in $\{50, 100, 200\}$ by subsampling ImageNet real training images and use 2x additional synthetic data of original ImageNet scale (2.4M) from our pipeline to train our models. Compared with baseline trained with real images, our approach shows significant improvement on overall accuracy.

The long-tailed version of ImageNet is constructed by truncating the original ImageNet training set. We use the exponential function [10] with different imbalance ratios (50, 100, and 200) to control the level of imbalance of real images. Likewise, we train all models for 100 epochs and use smaller batch sizes and learning rates as in low-data regime to train baseline models.

We define many-shot as classes with more than 800 real training images; medium-shot as classes with the number of real training images ranging from 300 to 800; and few-shot classes as classes with less than 300 training images. Results for many-shot, medium-shot, and few-shot classes are already reported in Table 2. Here, we additionally report the overall accuracy of each model in Table C for further reference.

C. Combination of Diversification Methods

As discussed in Section 3, our approach involves generating synthetic data with both contextual diversification (CD) and style diversification (SD). We present the results obtained using different combinations of these diversification techniques. Specifically, we leverage 2x synthetic data of original ImageNet scale for this study.

Table D showcases the performance of models trained with various combinations. Using only synthetic images with CD leads to models that struggle to generalize well to datasets like ImageNet-Sketch or ImageNet-Rendition. Conversely, utilizing only images with SD results in slightly lower performance in in-domain evaluation (indicated by underlined results). Notably, combining CD and SD yields the best performance for both in-domain and out-of-domain evaluations. Therefore, we keep the same amount of synthetic data with CD and SD for all our experiments.

D. Example of Diversified Generation Prompts

Our prompt diversification procedure involves contextual diversification (CD) and style diversification (SD). To better

	<u>ImNet</u>	ImNet-V2	Sketch	Rendition
2x CD	78.17	74.03	27.71	26.91
2x SD	77.95	73.92	30.41	29.67
1x CD + 1x SD	78.51	74.68	30.32	29.45

Table D. **Results with different combinations of diversification.** We use 2x synthetic data of original ImageNet scale and evaluate with different combinations of contextual diversification (CD) and style diversification (SD). ImageNet-val (underlined) is used for in-domain evaluation and others are for out-of-domain evaluation. Results show that using equal amount of synthetic data with CD and SD yields the best overall results.

understand our approach, we provide a list of examples of diversified prompts from CD and SD in this section.

Recall that contextual diversification prompts large language models to produce contextualized image descriptions featuring a particular object class in following four aspects: **foreground objects**, **background objects**, **lightning condition**, and **camera angle**. Descriptions of these aspects are joined together (each component is separated by comma) to form the text prompts in synthetic image generation. See below for examples:

GOLDFISH (N01443537)

goldfish swimming in a fish tank, bubbles, decorative plants, pebbles, artificial aquarium light, medium shot
goldfish in a fishbowl with a treasure chest decoration, table with scattered fish food, room light, low-angle shot
goldfish in a backyard pond, surrounded by rocks, trees, garden features, natural sunlight, wide shot
goldfish in a school swimming together, fish tank with other fish, underwater plants, daylight, panoramic shot

GOLDEN RETRIEVER (N02099601)

golden retriever swimming in a lake, blue sky, mountains in the distance, morning, wide shot
golden retriever playing with a Frisbee, open field, blue sky, afternoon, long shot
Golden retriever wearing a service dog vest, busy city street, daylight, medium shot
golden retriever wearing a birthday hat, party decorations, presents, indoor lightning, overhead shot

LEOPARD (N02128385)

resting leopard, tail curled, dense jungle foliage, trees,, dappled sunlight, medium shot
leopard crouching in hunting position, dense jungle, trees and foliage, golden hour, close-up shot
leopard drinking from a river, reflecting water, rocky terrain, distant mountains, harsh daylight, wide shot
leopard grooming itself, fallen tree trunk, colorful bird perched nearby, late afternoon sunlight, macro shot

PRETZEL (N07695742)

pretzel held in hand, a cup of coffee, a newspaper, natural daylight, close-up shot
pretzel with a drizzle of chocolate sauce, a plate of assorted desserts, dimmed lightning, medium shot
pretzel in a bakery display case, freshly baked bread, pastries, soft spotlight, close-up shot
pretzel being served with a side of sausages, traditional German beer garden, outdoor daylight, wide shot

The prompts with contextual diversification are then combined with the prefix “A *photograph of*” to generate photo-realistic synthetic images. On the other hand, the style diversification replaces *photograph* with each of the style keyword that is crawled from LLMs to form style diversified prompts. The list of style keywords is shown below:

STYLES FROM LLM

Sketch, Painting, Illustration, Digital rendering, Print, Comic-style depiction, Manga-style depiction, Pixel art representation, Tattoo design, Graffiti-style portrayal, Watercolor, Oil painting, Charcoal drawing, Pastel drawing, Stencil art, Collage, Mosaic, Silhouette, Pop art version, Sculpture, Origami, Embroidery, Quilt pattern, Stained glass design, Woodcut, Etching, Lithograph, Screen print, Relief carving, Bronze casting, Glass blowing, Ceramic pottery, Tapestry, Fresco, Mural, Doodle, Cartoon, Animation, 3D model, Wireframe model, CGI, Virtual reality model, Augmented reality model, Hologram, Gouache painting, Ink wash painting, Digital painting, Stencil graffiti, Airbrush art, Pointillism, Impasto painting, Engraving, Linocut, Marquetry, Papercut, Batik design, Cross-stitch pattern, Macramé design, Beadwork design, Sand sculpture

E. Synthetic Image Generation Details

We provide details of synthetic data generation in addition to the implementation details described in Section 4. Specifically, we set the guidance scale to 2.0 and use 50 sampling steps to generate synthetic images. Synthetic images are sampled at resolution of 1024x1024 and downsampled to 256x256 for storage. For faster generation, fp16 inference is used for all synthetic images.

F. Transfer Learning for Other Classification Tasks

To examine the quality of representation learned from our synthetic data, we further evaluate the transfer learning performance of our models on various classification tasks. Specifically, we evaluate on four datasets: Oxford Flowers [37], Oxford Pets [40], Food-101 [4], and Describable Textures [9]. Following the standard transfer learning evaluation protocol, we use both KNN and linear probing to evaluate transfer learning performance.

As shown in Table E, ResNet-50 models trained with diversified synthetic data demonstrate stronger performance

Training Data	Flowers	Pets	Food	DTD
KNN				
Real	66.75	88.06	52.25	57.18
Real + 6x Synthetic	67.26	90.27	55.44	61.70
Linear Probing				
Real	82.12	90.18	67.18	64.89
Real + 6x Synthetic	82.46	92.26	68.81	66.48

Table E. **Transfer Learning Evaluations.** We compare the transfer learning performance of a ResNet-50 model trained with only real ImageNet images, to a model trained with real + 6x synthetic ImageNet images. Results show that models trained with synthetic data (ours) demonstrate stronger capability to transfer to other tasks.

in transferring to other classification tasks under both k-nearest neighbor and linear probing evaluation. On average our model achieves +2.61% and +1.41% accuracy improvement with KNN and linear probing respectively.